Effect of dipolar and exchange interactions on magnetic blocking of maghemite nanoparticles

K. Nadeem [a,*], H. Krenn [a], T. Traussnig [b], R. Würschum [b], D.V. Szabó [c], I. Letofsky-Papst [d]

[a] Institute of Physics, Karl-Franzens University Graz, Universitätsplatz 5, A-8010 Graz, Austria
[b] Institute of Materials Physics, University of Technology Graz, A-8010 Graz, Austria
[c] Institute for Materials Research III, Karlsruhe Institute for Technology (KIT), 76021 Karlsruhe, Germany
[d] Institute for Electron Microscopy, University of Technology Graz, Steyrergasse 17, A-8010 Graz, Austria

ARTICLE INFO

Keywords:
Nanoparticle
Interparticle interaction
Dipolar
Exchange

ABSTRACT

Magnetic interparticle interactions compete with the magnetic blocking of ultrafine magnetic nanoparticles. We have prepared maghemite (γ Fe_2O_3) nanoparticles by microwave plasma synthesis as a loose powder and in compacted form. In ZFC/FC measurements, blocking temperature of the compacted sample C is larger than that of the powder sample P. The frequency dependence of AC susceptibility of the sample C shows a large shift of blocking temperature with increasing frequency. Vogel Fulcher law gives a large value of T_0 for the sample C. To get evidence of a possible spin glass freezing in both samples, scaling law fitting is applied to the AC susceptibility data. The value of the exponent ($z\nu$) of the critical slowing down dynamics fits to the spin glass regime for both samples. For the sample P, spin glass freezing occurs on the surface of individual nanoparticles, while in the sample C surface spin glass freezing is concomitant with a superspin glass formation as a consequence of coupling between particles. The sample C also shows an enhancement of coercivity due to dipolar interactions among the nanoparticles. Exchange interactions are attributed only to touching nanoparticles across their interfaces. All these measurements indicate the presence of strong interparticle dipolar interactions in the compacted sample C.

1. Introduction

Maghemite (γ Fe_2O_3) nanoparticles have been investigated intensively over the last years due to their potential applications in industry [1]. Nanoparticle magnetism is strongly influenced by interparticle dipolar (long range) or/and exchange (short range) interactions [2,3].

Maghemite (γ Fe_2O_3) is one of the ferrimagnetic materials ordered according to the inverse spinel structure with vacancies at the octahedral sites [4]. In spinel ferrite structure, oxygen forms an FCC lattice with cations distributed over tetrahedral (A) and octahedral (B) sites. The unit cell of a spinel ferrite consists of 32 oxygen, 16 trivalent iron and 8 divalent transition metal ions like in nickel ferrite ($NiFe_2O_4$) or cobalt ferrite ($CoFe_2O_4$). The spins at the tetrahedral and octahedral sites are anti parallel to each other. In maghemite (γ Fe_2O_3), Fe^{3+} ions occupy both tetrahedral (A) and octahedral (B) sites, the latter being only partly occupied by iron. The unit cell of maghemite (γ Fe_2O_3) is cubic with composition $(Fe_8^{3+})_A$ $[Fe_{40/3}^{3+}$ "□"$_{8/3}]_B$ O_{32} [4], where brackets ( ) and [ ] represent tetrahedral and octahedral sites, respectively, and "□" represents iron vacancies at octahedral sites. Due to these vacancies and competing interactions among spins located on different sublattices together with broken bonds, surface spins of maghemite nanoparticles experience frustration and disorder, which are ingredients for a possible spin glass state.

For magnetic nanoparticles, the blocking temperature is the temperature up to which the particle's magnetic moment keeps alignment to its anisotropy "easy" axis during experimental observation times. The blocking temperature of a nanoparticle depends on its surroundings and on interparticle interactions [5,6]. Consistently, the energy barrier of individual nanoparticles is strongly influenced by exchange and dipolar interactions. Kechrakos and Trohidou compared the influence of both exchange and dipolar interactions and their dependence on the particle concentration using Monte Carlo simulations [7]. Below the percolation limit both exchange and dipolar interactions raise the average blocking temperature due to enhanced interparticle interactions. García Otero et al. [8] have also reported an increase of blocking temperature with increasing nanoparticle concentration studied by Monte Carlo simulations, as well as diluted iron based nanoparticles dispersed in paraffin were experimentally studied by Vargas et al. [9]. Nunes et al. [10]

* Corresponding author. Tel.: +43 316 380 1625; fax: +43 316 380 9816.
E-mail address: kashif.nadeem@edu.uni-graz.at (K. Nadeem).

attributed such an increase of blocking temperature to dipolar interactions. Dai et al. [11] compared the surfactant coated maghemite nanoparticles in powder and compacted forms at different pressures and found an increase of blocking temperature with increasing pressure . They have neglected the contribution of exchange interaction since the nanoparticles were coated by a surfactant. They also found a negligible change of magnetic moment after compression. In our case, we have introduced exchange interactions by using bare maghemite nanoparticles without any surfactant. There is a conflict on the interpretation whether the energy barriers are increasing or decreasing with increasing inter particle interactions [12,13]. Dormann et al. [14,15] reported a model in which increasing interparticle interactions cause an increase of energy barriers. On the other hand, Mørup and Tronc [16] proposed a diminishing energy barrier with increasing interparticle interactions. Therefore we investigated the effects of both exchange and dipolar interactions on the magnetic properties of fine maghe mite nanoparticles in powdered and compacted forms. Our powder sample is highly mono disperse with a narrow particle size dis tribution and much larger coercivity than reported in the majority of published literature [9,10,17]. Fine maghemite nanoparticles either (i) enter the magnetic spin glass regime due to random freezing and frustration of surface spins or (ii) condense to a superspin glass state induced by random interparticle dipolar interactions [18 20].

2. Experiment

Fine maghemite nanoparticles have been prepared by micro wave plasma synthesis using a 2.45 GHz microwave equipment and $Fe(CO)_5$ as precursor material. The complete synthesis pro cess is described in detail in [21] and structural evaluation of the materials (made by the same process) is reported elsewhere [22]. The average particle size is 4 nm as proven by transmission electron microscopy. Samples are prepared in one batch and are subsequently divided into two lots, one as loose powder sample and the other as compacted sample applying a hand press machine. In the following, we will denote the powder and compacted sample as sample P and sample C, respectively. Transmission electron microscopy (TEM) was used (model number CM20 from FEI with 200 kV acceleration voltage and LaB_6 cathode) to analyze the average particle size distribution for supporting our findings from magnetometric measurements. Magnetic measurements were taken by using superconducting quantum interface device (SQUID) mag netometry (Quantum Design, MPMS XL 7) with maximum applied field of ± 7 T in the temperature range 4.2 300 K. The AC suscept ibility measurements were performed by the same magnetometer in the frequency range 0.1 1000 Hz and in the temperature range 4.2 300 K. The particles are highly mono disperse in diameter as evidenced by TEM and magnetic measurements. Due to the narrow size distribution, our prepared maghemite nanoparticles are good model substances for a reliable fit of experimental data to numerical simulations.

3. Results and discussion

Fig. 1(a,b) shows the transmission electron microscope (TEM) images of powder sample P at 20 and 2 nm scales. The particles are nearly spherical in shape. Inset of Fig. 1(a) shows the particle size distribution of sample P fitted by a log normal distribution function. The average particle size averaged over 134 evaluated particle diameters comes out to be 4 nm with standard deviation of $\sigma = 0.07$ from such a fit.

Fig. 2 shows experimental (blue down triangles) and simulated (red circles) zero field cooled/field cooled (ZFC/FC) measurements of powder sample P under 50 Oe applied field. For ZFC/FC experimental measurements, first the sample is cooled in zero field from room temperature to 4.2 K. Thereafter 50 Oe magnetic field is applied and magnetic moment is recorded with increasing temperature to get the ZFC curve. For the FC curve, the sample is cooled from 300 K under the same 50 Oe field and magnetic moment is recorded with decreasing temperature. The position of the observed peak in ZFC curve corresponds to the average magnetic blocking temperature (T_B) of the nanoparticles. Below the blocking temperature, the magnetocrystalline anisotropy energy ($K_{eff}V$, where K_{eff} is the effective anisotropy constant and V is the volume of the nanoparticle) dominates over the thermal energy k_BT and particles' magnetization is blocked along their individual "easy" anisotropy axes. Above the blocking temperature (T_B), the thermal energy is sufficient to deliberate the magnetic moments from their anisotropy axes and particles enter the super paramagnetic state. Recently, Bedanta and Kleemann [23] have reported a review article about the supermagnetism in nanomag nets, which will guide our investigations on powder and compacted maghemite nanoparticles. Sample P shows an average magnetic blocking temperature (T_B) at 49.5 K. The FC curve first increases and then becomes almost flat below 40 K. The flattening of FC curve is an indication of interparticle interactions or of spin glass like beha vior [20]. So it seems that the cause of the maximum in ZFC curve is not only due to pure core blocking but also substantially influenced by spin glass freezing.

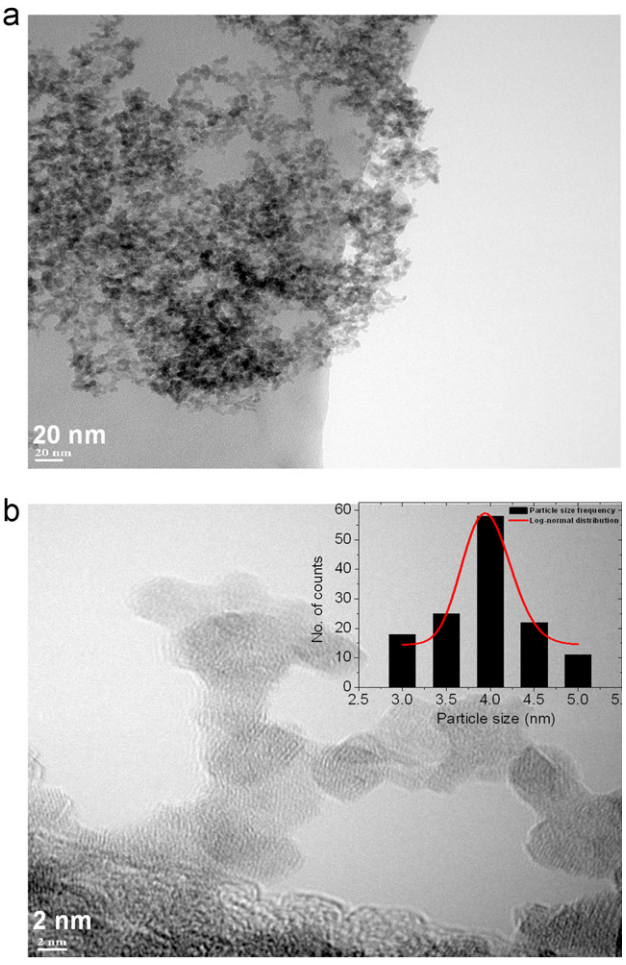

Fig. 1. Transmission electron microscopy of powder sample P at (a) 20 nm and (b) 2 nm scale. Inset in (b) shows particle size distribution fitted with log-normal distribution.

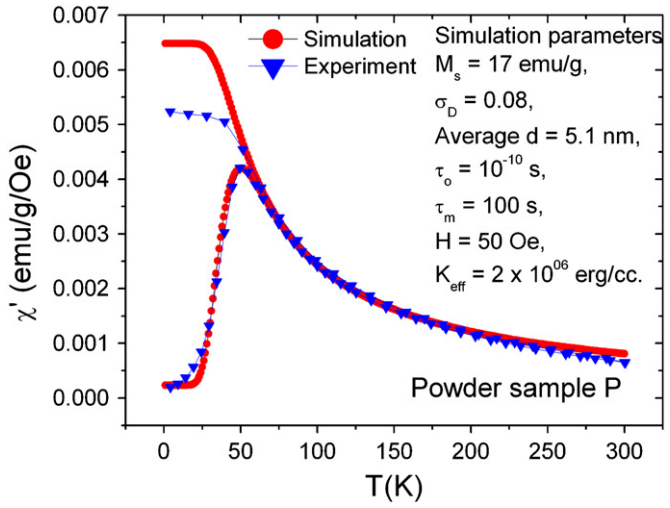

Fig. 2. Simulated (red circles) and experimental (blue down triangles) zero field cooled/field cooled measurements of powder sample P. (For interpretation of the references to color in this figure legend, the reader is referred to the web version of this article.)

The initial sharp increase and subsequent decrease of the ZFC curve of powder sample P demonstrate a narrow range of blocking temperatures concomitant with a narrow particle size distribution (which is also evident from TEM images, see Fig. 1(a,b)). Although powder sample P is uncoated and free of any surfactant, dipolar interactions are of minor importance as it is proved by the initial steep slope of ZFC curve and TEM analysis. Here from the steepness of ZFC curve of powder sample P, we can infer a very narrow size distribution of ± 0.08 evaluated by numerical fitting (red circles in Fig. 2) of ZFC/FC curves by a model for non interacting particles [24]. Fig. 2 shows simulation (red circles) of the ZFC/FC curves using Eqs. (3) and (4) for maghemite nanoparticles. For simulation, we have used the log normal distribution function of blocking temperatures T_B:

$$f(T_B)dT_B = \frac{1}{\sqrt{42\pi\sigma_{TB}^2}}\frac{1}{T_B}\exp\left(\frac{\ln^2 T_B/\langle T_B\rangle}{2\sigma_{TB}^2}\right)dT_B \quad (1)$$

Since the average blocking temperature $\langle T_B\rangle$scales with the average particle volume $\langle V\rangle = \pi\langle d\rangle^3/6$, we find:

$$\langle T_B\rangle = \frac{K_{eff}}{k_B \ln(\tau_m/\tau_0)}\langle V\rangle \quad (2)$$

According to the model for non interacting particles, the ZFC susceptibility is given by [24]

$$\chi_{ZFC}(T) = \frac{M_s^2}{3K_{eff}}\left[\ln\left(\frac{\tau_m}{\tau_0}\right)\int_0^T \frac{T_B}{T}f(T_B)dT_B + \int_T^\infty f(T_B)dT_B\right] \quad (3)$$

For a certain temperature T the first and second terms in Eq. (3) correspond to de blocked superparamagnetic and frozen blocked particles, respectively.

According to the same model, the FC susceptibility is given by [24]

$$\chi_{FC}(T) = \frac{M_s{}^2}{3K_{eff}}\ln\left(\frac{\tau_m}{\tau_0}\right)\left[\frac{1}{T}\int_0^T T_B f(T_B)dT_B + \int_T^\infty f(T_B)dT_B\right] \quad (4)$$

The best fit of the model to experimental ZFC/FC data yields $K_{eff} = 2\times10^6$ erg/cm^3 and an average particle size $\langle d\rangle = 5.1$ nm. The increased value of fitted K_{eff} with respect to bulk maghemite $K_{Bulk} = 4.7\times10^4$ erg/cm^3 [17] arises from an additional surface anisotropy contribution caused by frozen surface spins [25]. There is a difference between the experimental and fitted FC curves. The difference comes from the fact that the model assumes non interacting single domain nanoparticles. The experimental FC curve becomes flat immediately below the blocking peak but the fitted FC curve continues to increase and flattens at much lower temperatures. This flattening of the experimental FC curve just below the blocking peak is an indication of the presence of interparticle and/or surface spin glass freezing in the sample P.

Fig. 3 compares zero field cooled/field cooled (ZFC/FC) measurements of sample P (solid down triangles) with sample C (solid circles) under 50 Oe applied field. For compacted sample C, interparticle interactions cause an increase of the blocking temperature (85 K) due to increased dipolar and exchange interactions between small clusters consisting of pairs or triple of particles touching each other [7,9,10]. The magnetic moment (in units of emu/g) of compacted sample C is also less than powder sample P due to increased dipolar interactions in compacted sample C, in contrast to Dai et al. [11] who reported nearly no change of magnetic moment after compression of surfactant coated maghemite nanoparticles. Dipolar interactions are dominant among small sized nanoparticles due to less separation between the magnetic particles. The field cooled (FC) part also shows a distinct behavior of samples P and C. For non interacting nanoparticles, FC part shows a monotonic increase below the blocking peak [9,26]. Sasaki et al. [27] have reported how to distinguish between *superparamagnetism* and *superspin glass*. Below the blocking temperature T_B, they found a continuous increase of the FC curve for non interacting superparamagnetic ferritin and a nearly flat FC curve for Fe_3N nanoparticles frozen in a superspin glass state. Flatness and a slight dip in the field cooled (FC) magnetization are typical of spin glass systems. We have also found a flattening just below the blocking temperature for both samples (P and C) due to the presence of spin glass freezing and dipolar interactions; however sample C shows flatness immediately below the bifurcation point and a dip in the FC magnetization curve, which is attributed to spin glass behavior and more interparticle interactions [28,29]. The observation of memory, aging and rejuvenation effects after zero field cooling (ZFC) can also distinguish between superparamagnetic and spin glass states. The memory effect is specific for spin glasses and attributed to a tremendously enhanced correlation time by which the magnetic state is memorized for long stop and waiting times at a certain ZFC temperature below the freezing temperature (T_0). Our samples also exhibit memory effects under zero field cooled (ZFC) conditions (not shown here), which also proves the presence of spin glass behavior.

The relaxation time of blocked nanoparticles is determined by the energy barrier ($E_a = K_{eff}V$), thus the magnetic state of nanomagnets could be interrogated by frequency dependent AC susceptibility

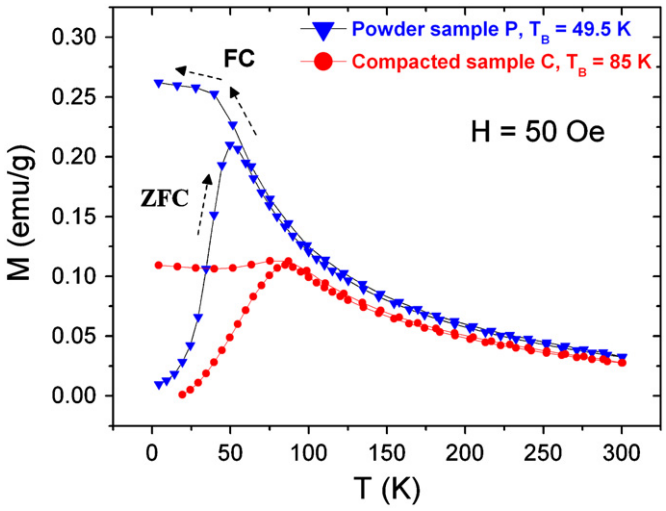

Fig. 3. Experimental zero field cooled/field cooled measurements of powder sample P and compacted sample C.

measurements. AC susceptibility contains information about the dynamics of the system. We measured the temperature dependent AC susceptibility for both samples to unravel the shift of T_B with the frequency of field excitation. The sample is cooled from room temperature in zero applied field to 4.2 K and then AC susceptibility is measured with increasing temperature. Fig. 4 shows the AC susceptibility of samples P and C at frequency f=0.1 Hz and amplitude A=5 Oe, respectively. Compacted sample C shows T_B peak at 89 K which is larger than the T_B peak of powder sample P at 58 K. The increase of T_B of compacted sample C is consistent with the ZFC/FC measurements (see Fig. 3).

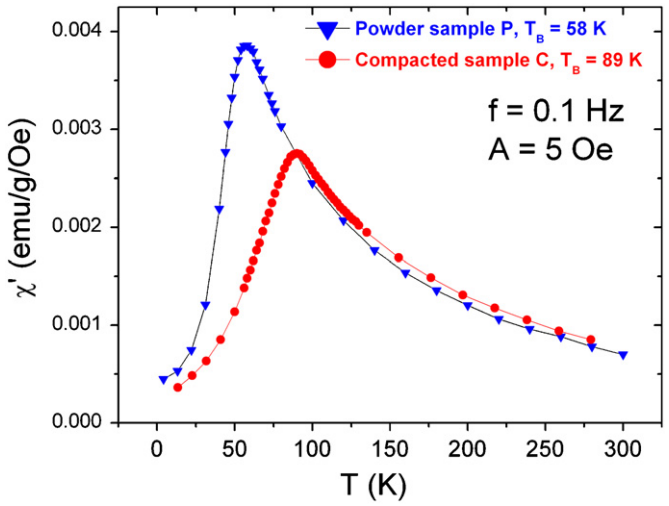

Fig. 4. AC susceptibility curves of samples P and C at frequency f 0.1 Hz and amplitude A 5 Oe.

Fig. 5(a) shows the frequency dependence of the in phase AC susceptibility of powder sample P in the frequency range 0.1 1000 Hz under magnetic field excitation with amplitude A=5 Oe. The blocking temperature T_B shifts from 58 to 72 K as the frequency is increased from 0.1 to 1000 Hz. Fig. 5(b) shows the frequency dependence of the in phase AC susceptibility of compacted sample C in the same frequency range. The plots show a shift of the blocking temperature with increasing frequency but the shift for the sample C is smaller (89 98 K) than the shift in powder sample P (58 72 K). Again, the smaller shift of T_B with an increasing frequency for the compacted sample C is due to increased interparticle interactions. Exchange and dipolar interactions are simultaneously operative in the compacted sample C, thus the system becomes stiffer causing smaller shift of T_B with increasing frequency.

Arrhenius law is valid for thermal excitation of single barrier blocked non interacting particles. The temperature dependence of the peak frequencies $f_p=\omega_p/2\pi$ of the AC susceptibility are subjected to an Arrhenius law fit (see Eq. (5)) for both samples and the result is shown in Fig. 6 (a) and (b) [4,5],

$$\tau = 1/\omega_p = \tau_0 e^{E_a/k_B T} \tag{5}$$

where τ_0 is the atomic spin flip time, E_a the activation energy and k_B the Boltzmann constant. The fit parameters τ_0 and E_a/k_B (in units of K) for both samples can be found in Table 1. For both samples, a very small unphysical values of τ_0 and an abnormally large activation energy parameter E_a/k_B has been found from the fit. The inadequate parameters call for a modified analysis using the Vogel Fulcher law [30] (Eq. (6)) with an additional parameter

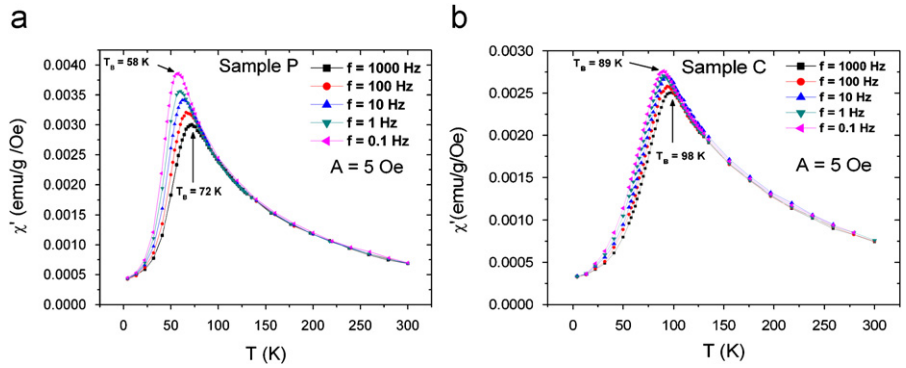

Fig. 5. Frequency dependence of AC susceptibility of (a) powder sample P and (b) compacted sample C.

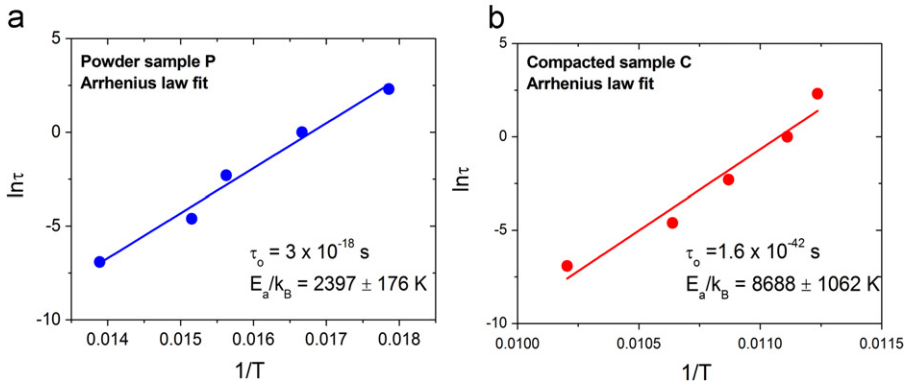

Fig. 6. Arrhenius law fit for (a) powder sample P and (b) compacted sample C.

T_0, representing the strength of interparticle interactions,

$$\tau = \frac{1}{\omega_p} = \tau_0 e^{E_a/k_B(T-T_0)} \quad (6)$$

Fig. 7 (a) and (b) show the results of a fit to the Vogel Fulcher law. The values of τ_0, E_a/k_B and T_0 from the best fits are given in Table 1. Spin flip time τ_0 and activation energy parameter E_a/k_B take reason able values for both samples. The increase of interaction parameter T_0=80 K for the compacted sample C as compared to the interaction parameter T_0=46 K for the powder sample P is a fingerprint for the enhanced interparticle interaction in the compacted sample C and compares very well with the DC and AC susceptibility data (see Figs. 3 and 4).

We have also calculated the relative variation of the blocking temperature peak ($\Delta T_B/T_B$) per frequency decade defined as parameter Ψ, [31,32]

$$\Psi = \frac{(\Delta T_B/T_B)}{\Delta \log_{10} f} \quad (7)$$

For non interacting particles this parameter takes the value $\Psi > 0.13$, for spin glasses $0.005 < \Psi < 0.05$, and for intermediate interactions $0.05 < \Psi < 0.13$ [31,32]. The parameter Ψ decreases with increasing strength of interparticle interactions. In our case we find 0.05 and 0.02 for powder sample P and compacted sample C, respectively. The decreased value of parameter Ψ for the compacted sample C indicates the presence of strong interparticle interactions and belongs to the spin glass phase. As it will be shown below for both samples, the fitted values of the dynamical critical exponent "zv" match with the spin glass regime.

Finally we have checked the possibility of spin glass freezing in both samples. There are basically two kinds of spin glass states in nanoparticles: (1) *superspin glass* and (2) *surface spin glass*. Nanoparticles with or without non magnetic matrix can get collectively frozen at low temperatures due to interparticle dipolar interactions known as super spin glass state. Bedanta et al. [33] recently reported a study about interparticle interaction in CoFe nanoparticles embedded in a non magnetic matrix (Al_2O_3) in the form of discontinuous metal insulator multilayers (DMIMs). They found *superparamagnetic* relaxation for low nano particle density due to the absence of strong dipolar interactions and *superspin glass* ordering at higher particle concentrations, which is attributed to strong dipolar interactions among the nanoparticles. Above certain nanoparticle concentration, they found a ferromagnetic like state called superferromagnetism (SFM) due to less interparticle distance and strong interparticle interactions [28]. We have not found a superferromagnetic (SFM) state in our dense compacted sample C (which is evident by the reduction of magnetic moment in ZFC/FC magnetization of sample C as compared to sample P as shown in Fig. 3), which may be due to the fact that the interparticle interactions are not strong enough to align the nanoparticles in one direction. Spins on the individual nanoparticle surfaces can also undergo a spin glass phase transition at low temperature, which is known as a surface spin glass state. Like in bulk spin glasses, disorder and frustration on the surface of fine nanoparticles are necessary prerequisites for a possible spin glass freezing [34]. Surface spin glass behavior is more pronounced in fine nanoparticles due to an increased surface to volume ratio. Winkler et al. [35] have recently reported spin glass behavior in antiferromagnetic nickel oxide (NiO) nanoparticles, Peddis et al. [36] in fine cobalt ferrite ($CoFe_2O_4$) nanoparticles and attributed the observed spin glass phase to a random freezing of surface spins.

We have fitted the dynamic scaling law to the AC susceptibility data of both the samples as shown in Figs. 8 and 9. In critical dynamics the following time scaling rule holds [37]:

$$\tau(f) = \tau^* \left[\frac{T_0}{T_s(f) \quad T_0}\right]^{zv} \quad (8)$$

where $\tau(f)$ is the frequency dependent relaxation time of spins, τ^* is related to the coherence time of coupled individual "atomic" spins in the nanoparticle, T_0 is the static transition (freezing) temperature and $T_s(f)$ is the frequency dependent freezing tem perature. We have taken $T_s(f)$ as the maximum of AC suscept ibility curve. Scaling law indicates that there is critical slowing down of relaxation times near the transition temperature T_0.

First we will discuss a possible spin glass behavior in the powder sample P. Fitting of scaling law (Eq. (8)) gives reasonable values for the critical exponent zv and the coherence time τ^* for powder sample P: zv=10.6 and $\tau^* = 6 \times 10^{-07}$ s, as shown in Fig. 8. The value of critical exponent zv=10.6 is typical of spin glass behavior (ranging 4 12 for different spin glass sys tems) [31,38]. The higher value of spin flip time τ^* is due to quenched atomic relaxation of frozen surface spins. A spin glass

Table 1
Values of fitted parameters for models as described in Eqs. (5), (6), and (8).

Model	Parameters	Sample P (powder)	Sample C (compacted)
Arrhenius	τ_0 (s)	3×10^{-18}	1.6×10^{-42}
	E_a/k_B (K)	2397 ± 176	8688 ± 1062
Vogel–Fulcher	τ_0 (s)	5.2×10^{-07}	9.7×10^{-08}
	E_a/k_B (K)	203 ± 16	164 ± 5.7
	T_0 (K)	46	80
Scaling	τ^* (s)	6×10^{-07}	1.5×10^{-10}
	zv	10.6 ± 0.9	8.1 ± 0.9
	T_0 (*K*)	48	85

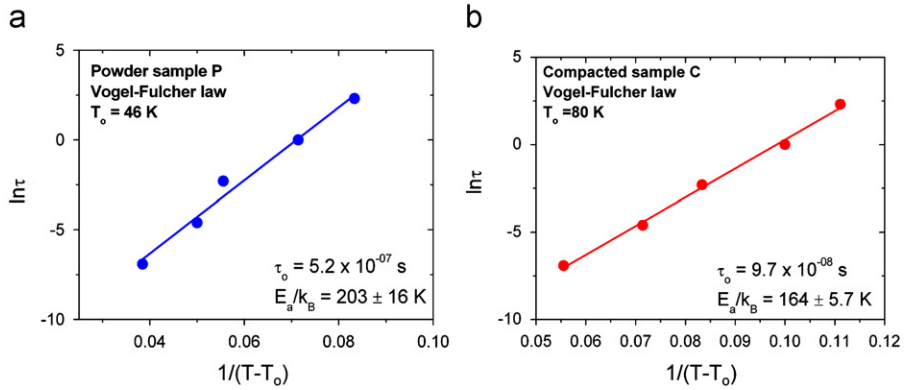

Fig. 7. (a) Vogel–Fulcher law fit for (a) powder sample P and (b) compacted sample C.

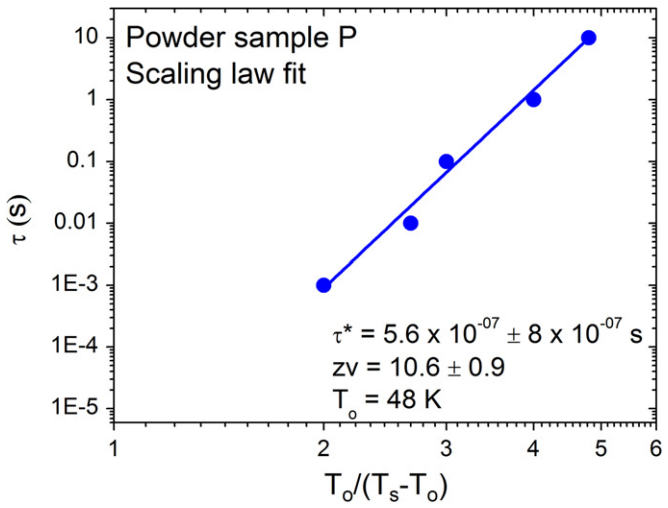

Fig. 8. Scaling law fit for powder sample P.

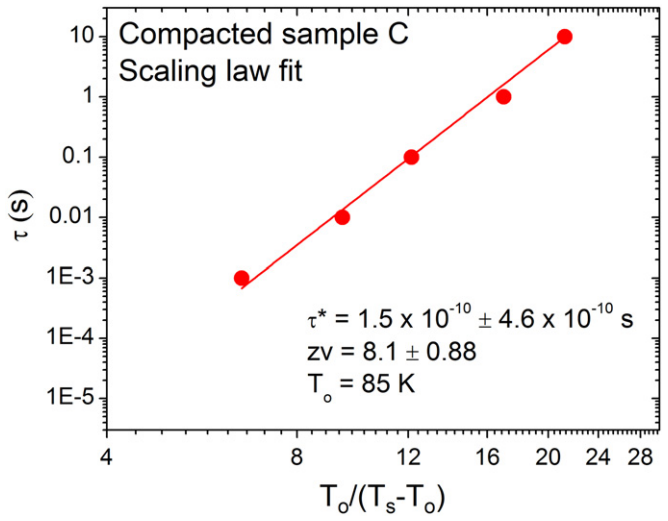

Fig. 9. Scaling law fit for compacted sample C.

transition of maghemite nanoparticles of sizes 9 10 nm has been reported by Martínez et al. [20] and was attributed to random freezing of frustrated surface spins. Powder sample P shows a very narrow blocking temperature distribution and mild inter particle interactions as compared to compacted sample C. Thus the spin glass behavior in powder sample P can be explained by surface spin glass freezing. Now we will discuss the spin glass freezing in compacted sample C. Fig. 9 shows fitting of scaling law fit for compacted sample C. The value of critical exponent $zv=8.1$ for compacted sample C also falls in the spin glass regime. In compacted sample C, we have an extra contribution of superspin glass behavior (due to dipolar interactions) in addition to surface spin glass, which is also evident by immediate flatness and dip of FC curve for sample C as shown in Fig. 3 [18,19]. The value of the coherence time $\tau^*=1.5\times 10^{10}$ s for compacted sample C is much smaller than the value of powder sample P ($\tau^*=6\times 10^{07}$ s). In case of compacted sample C, two or three particles are touching each other due to compaction and these surface spins become coupled via exchange interaction at the touching points. These exchange coupled surface spins at the contact point are atomic like (because collective 3 dimensional magnon modes can be excited) and relax much faster than the blocked disordered spins in case of frozen non touching surface spins.

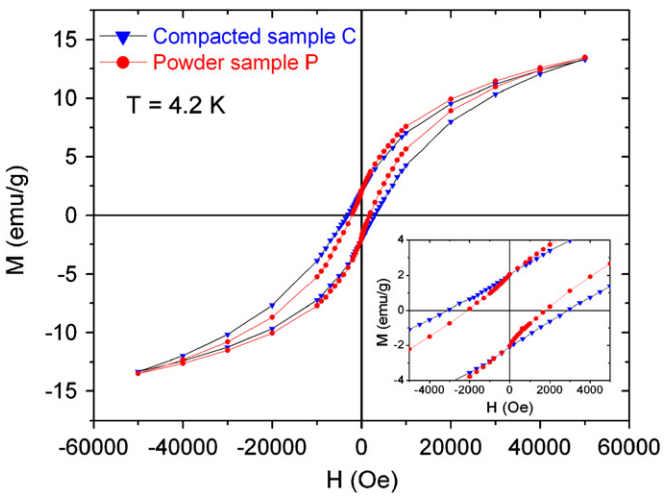

Fig. 10. Hysteresis loops of both powder and compacted samples at temperature T 4.2 K.

Coercivity is also an important parameter that can be influ enced by exchange or/and dipolar interactions. Fig. 10 shows hysteresis loops of samples P and C with a maximum applied field of ± 5 T measured at temperature $T=4.2$ K. The coercivity shows an increase for compacted sample C ($H_c=3008$ Oe) as compared to powder sample P ($H_c=1940$ Oe). Blanco Mantecon and O'Grady [39] reported an increase of coercivity with increasing interparticle interactions. Verdes et al. [40] presented a computa tional model in which they showed an increase of coercivity with increasing interparticle interactions. The increase of coercivity of compacted sample C is due to an increase of energy barriers caused by dominant dipolar interactions [41]. Exchange interac tions are much more localized between the touching nanoparti cles at the surface and do not influence the dipolar interactions among the nanoparticle core spins. The saturation magnetization (M_s) (in units of emu/g) of both the samples is almost equivalent due to quench of dipolar interactions by high external magnetic field. Saturation magnetization of both samples is less than the saturation magnetization of bulk maghemite: M_s (bulk)=80 emu/g [17,42]. The decrease of M_s with the diameter of ferrite nanopar ticles is a very well known effect, since the surface to volume ratio becomes of significant importance. The atoms on the surface have truncated bonds and less coordination neighbors, thus their mutual exchange interaction is reduced. The surface magnetic anisotropy induces a radial easy axis on the nanoparticle surface. Kodama et al. [25] have proposed a model for disorder induced surface spin freezing in ferrite nanoparticles. Therefore the occurrence of lower M_s for ferrite nanoparticles is due to the disordered surface spins. Frozen spins at the surface are the reason that the hysteresis loop is not saturated even for fields up to ± 5 T.

4. Conclusions

We have studied the effects of exchange and dipolar interac tions on magnetic properties of very small (4 nm) maghemite nanoparticles prepared by microwave plasma synthesis. The prepared maghemite nanoparticles show a highly mono disper sive size distribution with a narrow blocking temperature dis tribution as evidenced by TEM analysis and ZFC susceptibility measurements. These mono disperse nanoparticles are promising candidates for a quantitative comparison of experimental mag netic studies with theoretical simulations. Presence of high coercivity and open loop hysteresis at high fields ± 5 T is due to large surface

spin disorder and spin glass freezing. Simulated and experimental ZFC/FC measurements show discrepancy in the FC curve due to the fact that the model assumes only non interacting single domain nanoparticles without any surface effects. Fitted anisotropy constant (K_{eff}) comes out larger than the corresponding bulk value which is attributed to an additional contribution from surface anisotropy. Compacted sample shows an increase of blocking temperature in both ZFC/FC and AC susceptibility measurements due to an increase of interparticle interactions. Thermal activation according to the Arrhenius law gives unphysical results of spin flip time and activa tion energy parameter. Fits to the Vogel Fulcher law could relax the unphysical values of fitting parameters and provide a reasonable magnitude for the atomic spin flip time of both the samples. The increase of the interaction parameter T_0 of compacted sample with respect to the powder sample is attributed to stronger interparticle interactions in compacted sample. The parameter Ψ independent of any model is correspondingly reduced for the compacted sample. A possible spin glass freezing is checked by fitting dynamic scaling law. Both samples yield reasonable values of critical exponent ($z\nu$) in the spin glass regime. The existence of spin glass system in powder form is due to surface spin glass freezing, while in compacted sample, there is an additional contribution of superspin glass formation in combination with surface spin glass freezing. Dipolar interactions among nanoparticles are responsible for superspin glass freezing in the compacted sample. To explain the fast relaxation time in compacted sample, the mechanism of very local exchange interac tions between touching nanoparticles is adopted. This should be not confused with the random anisotropy model, in which collective alignment of the particle magnetization is driven by strong inter particle exchange interaction, which yields an average lowering of anisotropy barrier and opposite shift of blocking temperature in contrast to our experimental findings. Coercivity is increased in compacted sample due to large energy barriers, which in turn signifies the dominance of dipolar interactions in compacted sample. All these measurements show the presence of substantial dipolar interactions between nanoparticles in the compacted sample, whereas in the powder sample mutual interactions are superseded by effects of surface spin glass freezing of (nominally uncoupled) individual particles. From our investigations, we found evidence that the nanoparticles in the dense sample (sample C) are not exchange coupled (except small clusters of 2 or 3 coupled nanoparticles), but are rather organized in a dipolar superspin glass system.

Acknowledgements

K. Nadeem acknowledges the Higher Education Commission (HEC) of Pakistan for providing foreign PhD scholarship. The authors thank the Austrian Science Fund (FWF) (national funds) for granting the network projects (NFN) S10407 N16, S10405 N16 and the NAWI Graz GASS cooperation project.

References

[1] A.S. Teja, P.Y. Koh, Prog. Cryst. Growth Charact. Mater. 55 (2009) 22–45.
[2] J.L. Dormann, R. Cherkaoui, L. Spinu, M. Nogues, F. Lucari, F. Dorazio, D. Fiorani, A. Garcia, E. Tronc, J.P. Jolivet, J. Magn. Magn. Mater. 187 (1998) 139–144.
[3] M. Uhl, B. Siberchicot, J. Phys. Condens. Matter 7 (1995) 4227.
[4] R.M. Cornell, U. Schwertman, The Iron Oxides, Structure, Properties, Reactions, Occurrences and Uses, Wiley–VCH, Weinheim, 2003.
[5] L. Néel, Ann. Geophys. 5 (1949) 99.
[6] W.F. Brown, Phys. Rev 130 (1963) 1677.
[7] D. Kechrakos, K.N. Trohidou, J. Magn. Magn. Mater. 262 (2003) 107.
[8] J. García-Otero, M. Porto, J. Rivas, A. Bunde, Phys. Rev. Lett. 84 (2000) 167.
[9] J.M. Vargas, W.C. Nunes, L.M. Socolovsky, M. Knobel, D. Zanchet, Phys. Rev. B 72 (2005) 184428.
[10] W.C. Nunes, F. Cebollada, M. Knobel, D. Zanchet, J. Appl. Phys. 99 (2006) 08N705.
[11] J. Dai, J.Q. Wang, C. Sangregorio, J. Fang, E. Carpenter, J. Tang, J. Appl. Phys. 87 (2000) 7397–7399.
[12] J.L. Dormann, D. Fiorani, E. Tronc, J. Magn. Magn. Mater. 202 (1999) 251.
[13] M.F. Hansen, S. Mørup, J. Magn. Magn. Mater. 184 (1998) 262–274.
[14] J.L Dormann, L. Bessais, D. Fiorani, J. Phys. C: Solid State Phys. 21 (1988) 2015.
[15] J.L. Dormann, L. Spinu, E. Tronc, J.P. Jolivet, F. Lucari, F. D'Orazio, D. Fiorani, J. Magn. Magn. Mater. 183 (1998) 255.
[16] S. Mørup, E. Tronc, Phys. Rev. Lett. 72 (1994) 3278.
[17] D. Fiorani, A.M. Testa, F. Lucari, F. D'Orazio, H. Romero, Physica B 320 (2002) 122–126.
[18] D. Parker, V. Dupuis, F. Ladieu, J.P. Bouchaud, E. Dubois, R. Perzynski, E. Vincent, Phys. Rev. B 77 (2008) 104428.
[19] S. Nakamae, Y. Tahri, C. Thibierge, D.L. Hôte, E. Vincent, V. Dupuis, E. Dubois, R. Perzynski, J. Appl. Phys. 105 (2009) 07E318.
[20] B. Martínez, X. Obradors, L.I. Balcells, A. Rouanet, C. Monty, Phys. Rev. Lett. 80 (1998) 181.
[21] D. Vollath, D.V Szabó, J. Nanopart. Res. 8 (2006) 417–428.
[22] D. Vollath, D.V. Szabó, R.D. Taylor, J.O. Willis, J. Mater. Res. 12 (8) (1997) 2175–2182.
[23] S. Bedanta, W. Kleemann, J. Phys. D: Appl. Phys. 42 (2009) 013001.
[24] J.C. Denardin, A.L. Brandl, M. Knobel, P. Panissod, A.B. Pakhomov, H. Liu, X.X. Zhang, Phys. Rev. B 65 (2002) 064422.
[25] R.H. Kodama, A.E. Berkowitz, E.J. McNiff, S. Foner, Phys. Rev. Lett. 77 (1996) 394.
[26] S. Mitra, K. Mandal, A.P. Kumar, J. Magn. Magn. Mater. 306 (2006) 254–259.
[27] M. Sasaki, P.E. Jönsson, H. Takayama, H. Mamiya, Phys. Rev. B 71 (2005) 104405.
[28] O. Petracic, X. Chen, S. Bedanta, W. Kleemann, S. Sahoo, S. Cardoso, P.P. Freitas, J. Magn. Magn. Mater. 300 (2006) 192–197.
[29] D. Peddis, C. Cannas, A. Musinu, G. Piccaluga, J. Phys. Chem. C 112 (2008) 5141–5147.
[30] S. Shtrikman, E.P. Wolfarth, Phys. Lett. 85A (1981) 467.
[31] J.A. Mydosh, Spin Glasses, Taylor and Francis, Washington, 1993.
[32] J.L. Dormann, D. Fiorani, E. Tronc, Adv. Chem. Phys. 98 (1997) 283.
[33] S. Bedanta, O. Petracic, X. Chen, J. Rhensius, S. Bedanta, E. Kentzinger, U. Rücker, T. Brückel, A. Doran, A. Scholl, S. Cardoso, P.P. Freitas, W. Kleemann, J. Phys. D: Appl. Phys. 43 (2010) 474002.
[34] K. Binder, A.P. Young, Rev. Mod. Phys. 58 (1986) 801.
[35] E. Winkler, R.D. Zysler, M. Vasquez Mansilla, D. Fiorani, D. Rinaldi, M. Vasilakaki, K.N. Trohidou, Nanotechnology 19 (2008) 185702.
[36] D. Peddis, C. Cannas, G. Piccaluga, E. Agostinelli, D. Fiorani, Nanotechnology 21 (2010) (2010) 125705.
[37] P.C. Hohenberg, B.I. Halperin, Rev. Mod. Phys. 49 (1977) 435.
[38] K.H. Fischer, J.A. Hertz, Spin Glasses, Cambridge University Press, Cambridge, 1991.
[39] M. Blanco-Mantecon, K. O'Grady, J. Magn. Magn. Mater. 296 (2006) 124.
[40] C. Verdes, B. Ruiz-Diaz, S.M. Thompson, R.W. Chantrell, A. Stancu, Phys. Rev. B 65 (2002) 174417.
[41] D. Caruntu, G. Caruntu, C.J. O'Connor, J. Phys. D: Appl. Phys. 40 (2007) 5801.
[42] M.D. Coey, Phys. Rev. Lett. 27 (1971) 1140.